J. Fluid Mech. (2006), *vol.* 558, *pp.* 103–111. © 2006 Cambridge University Press
doi:10.1017/S0022112006000188 Printed in the United Kingdom

Flow behaviour of dielectric liquids in an electric field

By H. B. ZHANG, M. J. EDIRISINGHE† AND S. N. JAYASINGHE

Department of Mechanical Engineering, University College London, Torrington Place, London WC1E 7JE, UK

(Received 20 October 2005 and in revised form 27 February 2006)

A family of 10 silicone oils with electrical conductivity $\sim 10^{-13}\,\mathrm{S\,m^{-1}}$ (a regime hitherto systematically unexplored) and viscosities ranging from 1 to 2000 mPa s have been subjected to an electrical field of up to $1.5\,\mathrm{kV\,mm^{-1}}$ during flow from a needle. The flow behaviour of these liquids is investigated experimentally in the flow rate regime 10^{-8}–$10^{-12}\,\mathrm{m^3\,s^{-1}}$ and we analyse the results using the Ohnesorge number. Due to the low electrical conductivity and high electrical relaxation time of the silicone oils, only unsteady transient jets were found. The onset of this type of jetting has been defined using current measurements and, in contrast to conducting liquids, the non-dimensional jet diameter increases with increase in Ohnesorge number. The time elapsed between the start and finish of jetting increases with increasing Ohnesorge number.

1. Introduction

The flow of liquids in a high-voltage-driven electric field has received much attention in the last two decades because of the phenomenon of jetting and droplet generation, which have numerous applications in agriculture, bioengineering, environmental engineering and materials science (Fenn *et al.* 1989; Gomez *et al.* 1998; Jayasinghe & Edirisinghe 2002). Viscosity and electrical conductivity are two major parameters of the jet and droplet generation process. However, most of the liquids investigated have an electrical conductivity in the range of 10^{-3} to $10^{-6}\,\mathrm{S\,m^{-1}}$ and viscosities <140 mPa s. Liquids having a lower electrical conductivity have been studied, e.g. mineral oil ($1.7\times10^{-7}\,\mathrm{S\,m^{-1}}$) and silicone oils ($10^{-12}\,\mathrm{S\,m^{-1}}$), but by submerging a charge carrier having a radius $<1\,\mu\mathrm{m}$ into the liquid to generate enough charge (Galicki, Berezin & Chang 1996; Balachandran & Machowski 1998).

Decreasing the electrical conductivity to the dielectric regime ($\leqslant 10^{-12}\,\mathrm{S\,m^{-1}}$) makes a fundamental difference to the physical principle governing the process. That is, in such instances, the electrical relaxation time exceeds the hydrodynamic time and, therefore, although classical electrohydrodynamic atomization (EHDA) cannot prevail (Ganan-Calvo, Davila & Barrero 1997), jetting and droplet generation is possible (Jayasinghe & Edirisinghe 2004*a*, *b*). As a family of liquids, silicone oils can have a wide range of viscosity while other properties such as electrical conductivity, relative permittivity and surface tension are virtually constant. In addition most silicone oils are dielectric and allow the systematic exploration of the conductivity regime

† Author to whom correspondence should be addressed: m.edirisinghe@ucl.ac.uk

Samples	Viscosity η (mPa s)	Density ρ (kg m^{-3})	Surface tension σ (mN m^{-1})	Relative permittivity ε	DC electrical conductivity κ (S m^{-1})
S1	0.8	818	17.4	2.29	2×10^{-13}
S2	4.6	920	19.7	2.59	1×10^{-13}
S3	9.3	934	20.1	2.64	1×10^{-13}
S4	19.0	949	20.6	2.68	1×10^{-13}
S5	48.0	960	20.8	2.71	1×10^{-13}
S6	96.0	960	20.9	2.73	1×10^{-13}
S7	194.0	970	21.0	2.74	1×10^{-13}
S8	485.5	971	21.1	2.75	1×10^{-13}
S9	971.0	971	21.2	2.75	1×10^{-13}
S10	1942.0	971	21.2	2.76	1×10^{-13}

TABLE 1. Properties of the silicone oils.

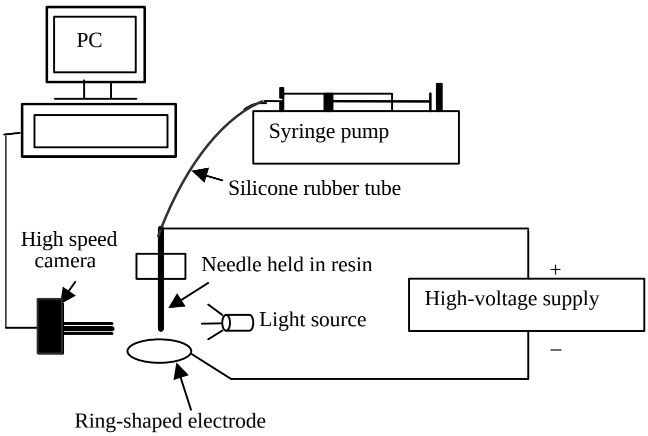

FIGURE 1. Experimental setup used in this work.

$\leqslant 10^{-13}$ S m^{-1} while viscosity is varied from 1 to 2000 mPa s, a range of significant importance to materials processing (Jayasinghe & Edirisinghe 2005). This is the subject of the present investigation, which is relevant to the study of the discharge of isolated microdrops of low-electrical-conductivity and high-viscosity-liquids raised to the Rayleigh limit (Li, Tu & Ray 2005).

2. Experimental details

The samples of silicone oils used in this investigation were obtained from Univar Ltd., Greenwich, UK. The physical and electrical properties of the samples such as density (ρ), viscosity (η), surface tension (σ), electrical conductivity (κ) and relative permittivity (ε) were provided by the supplier table 1.

The experimental setup used in this work is shown in figure 1. The stainless steel needle, which has an orifice diameter of 330 μm, was held in epoxy resin and connected to the positive terminal of the power supply (Glassman Europe Ltd., Tadley, UK). The liquid was delivered to the needle through a silicone rubber tube by a syringe pump (HARVARD Apparatus Ltd., Edenbridge, UK). A ring-shaped electrode (internal diameter 15 mm and external diameter 19 mm) was earthed and held 10 mm below

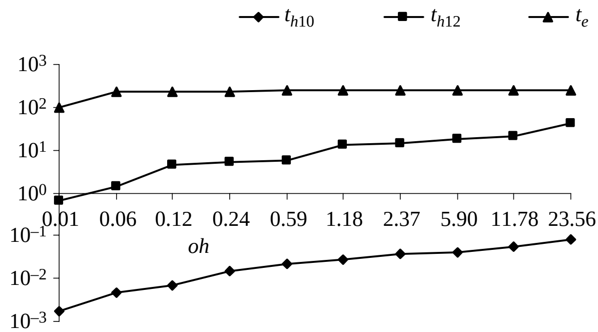

FIGURE 2. Variation of hydrodynamic time (t_h) at different flow rates and electrical relaxation time (t_e) with Ohnesorge number.

the needle. A high-speed camera (Weinberger AG, Dietikon, Switzerland) was used to study the oil exiting the needle. The experiments were carried out in the flow rate (Q) regime of 10^{-8} to $10^{-12}\,\mathrm{m^3\,s^{-1}}$ and the applied voltage was varied up to 15 kV. The flow rates quoted refer to the rate of liquid pumped to the meniscus. The definition of the flow rate is particularly important in the present work as in an unsteady scenario the flow rate into the liquid meniscus could be quite different to the flow rate delivered via the jet.

The charging current was measured by connecting a Fluke 189 digital multimeter to the power supply according to specifications given by the manufacturer of the power supply used. Three current readings were taken for each silicone oil with the applied voltage set at 10 kV at flow rates of $10^{-10}\,\mathrm{m^3\,s^{-1}}$ and $10^{-12}\,\mathrm{m^3\,s^{-1}}$, conditions which caused the onset of unstable transient jetting reported in this paper.

3. Results and analysis

In the Rayleigh break-up or capillary break-up process, the Ohnesorge number $oh = \eta/(\rho\sigma l_0)^{1/2}$ and capillary time $t_c = (\rho l_0^3/\sigma)^{1/2}$ are the two relevant non-dimensional parameters (Lopez-Herrera & Ganan-Calvo 2004; McKinley 2005), where l_0 is the characteristic length, which is taken as 330 μm, the orifice diameter. The family of silicone oils investigated in this work has a very low electrical conductivity ($\sim 10^{-13}\,\mathrm{S\,m^{-1}}$), a similar density, relative permittivity and surface tension, parameters which affect their flow in an electric field (Rosell-Llompart & Fernández de la Mora 1994; Chen & Pui 1997; Ku & Kim 2002). Therefore, in our work the Ohnesorge number represents the viscosity effects and is selected as the basis for the analysis of the results.

Using the values in table 1, in the flow rate range of 10^{-8}–$10^{-12}\,\mathrm{m^3\,s^{-1}}$, if the jet length takes the value of 0.01 m (the distance between the tip of the needle and ground electrode), the relaxation time t_e is in the range of 100–240 s, while the hydrodynamic time t_{h10} and t_{h12} at flow rates of $10^{-10}\,\mathrm{m^3\,s^{-1}}$ and $10^{-12}\,\mathrm{m^3\,s^{-1}}$ shown in figure 2 are in the range of 0.001–40. Here, $t_e = \varepsilon\varepsilon_0/k$, where ε_0 is the permittivity constant of vacuum ($8.85 \times 10^{-12}\,\mathrm{F\,m^{-1}}$) and $t_h = Lj_d^2/Q$, where L is the jet length and j_d is the jet diameter. Therefore, $t_e \gg t_h$, and classical EHDA does not take place in these liquids. At $10^{-9}\,\mathrm{m^3\,s^{-1}}$, all the silicone oils investigated in this work exhibited dripping as illustrated in figure 3. At higher flow rates (e.g. $10^{-8}\,\mathrm{m^3\,s^{-1}}$), t_h is reduced even further and therefore the difference between t_e and t_h increases and EHDA is even more

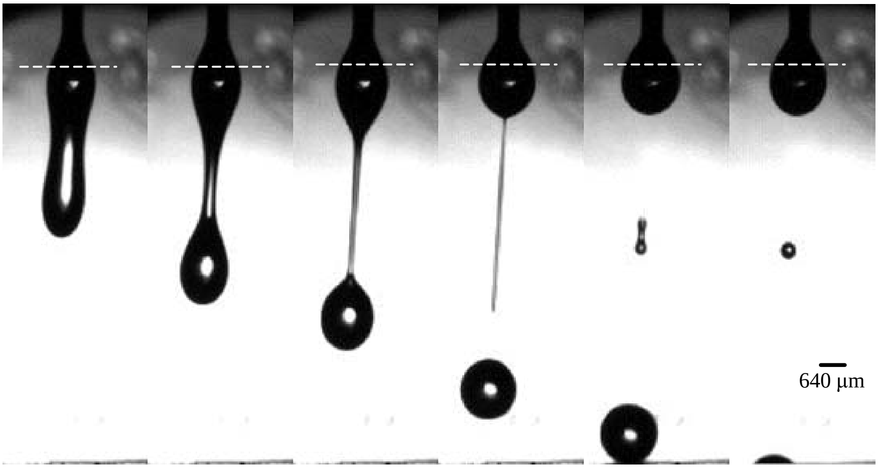

FIGURE 3. Dripping in sample S5 (see table 1) at 10^{-9} m^3 s^{-1} and 10 kV; the dotted line indicates the exit of the needle.

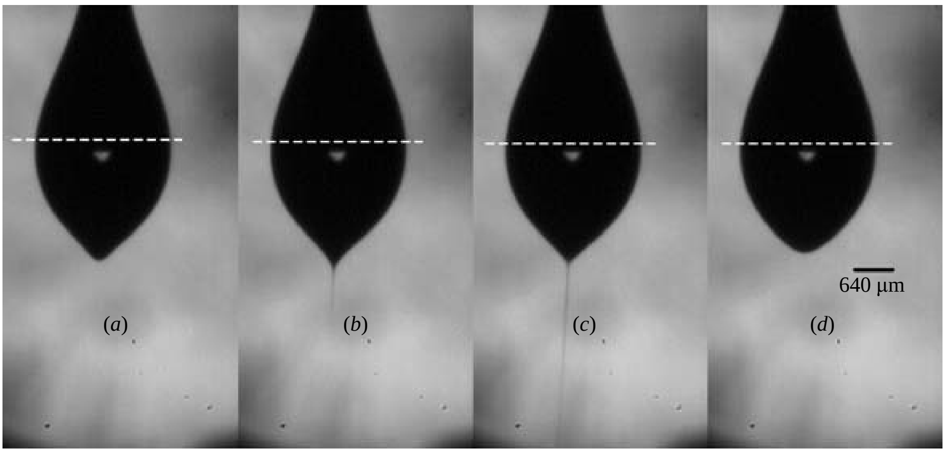

FIGURE 4. Unsteady jetting in sample S2 at 10^{-10} m^3 s^{-1} and 10 kV; the dotted line indicates the exit of the needle. The frames were taken in sequence (every 1.5 ms) and indicate (*a*) jetting about to start; (*b*) and (*c*) jetting; (*d*) no jet.

unlikely. In fact, it was not possible to initiate jetting in the entire range of applied voltages (up to 15 kV) and the flow rate regime 10^{-8} to 10^{-9} m^3 s^{-1}.

At 10^{-10} m^3 s^{-1}, all samples were found to be dripping at an applied voltage <9 kV. Above 9 kV, unsteady transient jets were initiated in all the samples (e.g. figure 4). At 10^{-12} m^3 s^{-1}, the samples generate such jets at a lower applied voltage of 6 kV below which dripping takes place. This jet evolves from a ball–cone (Jayasinghe & Edirisinghe 2004*b*) formed at the tip of the needle and a fine jet is ejected from the apex of the cone (figure 5). We use the more appropriate term 'unsteady' rather than 'unstable' to describe these jets. This is because charged or uncharged capillary jets are unstable, breaking up in a normal or lateral unstable mode and in EHDA, in the widely quoted stable cone–jet mode, steady jets originate from the vertex of a conical meniscus. In contrast, in the work reported here steady jets are not found and only unsteady jets prevail.

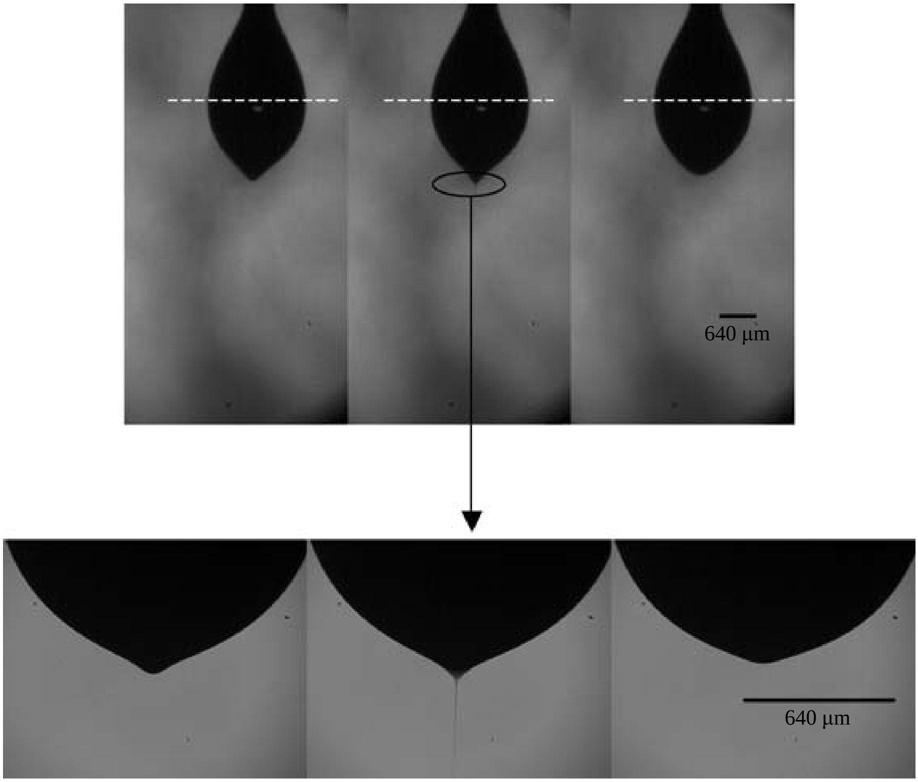

FIGURE 5. The formation of the ball–cone and unsteady jetting in S1 at $10^{-10}\,m^3\,s^{-1}$ and 10 kV.

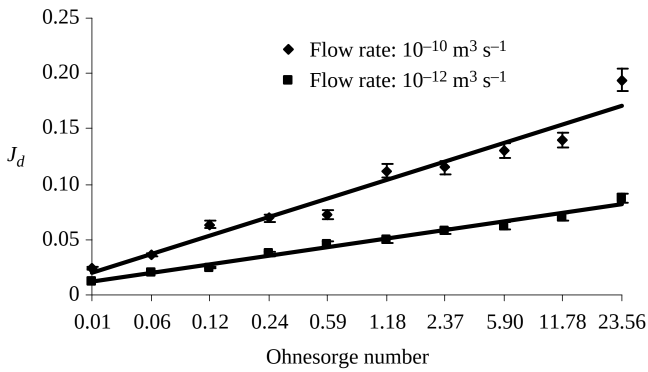

FIGURE 6. The variation of non-dimensional jet diameter as a function of the Ohnesorge number.

Figure 6 shows the relationship between non-dimensional jet diameter $J_d = j_d/l_0$ and Ohnesorge number for flow rates of 10^{-10} and $10^{-12}\,m^3\,s^{-1}$ at 10 kV. The jet diameter j_d was measured at the point just before the jet breaks up. The measurements were carried out using image processing software (Image Pro-Express) and calibrated using an image of known diameter. This measurement is accompanied by an error bar calculated using five independent readings. It was found that with increase in Ohnesorge number the non-dimensional jet diameter increases. At lower flow rates,

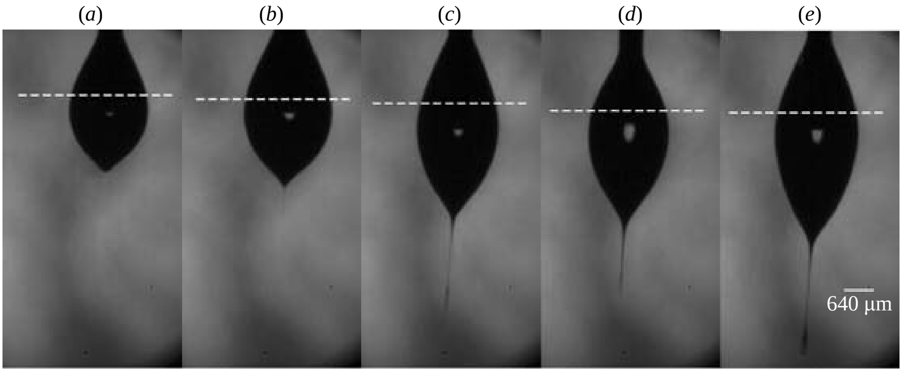

FIGURE 7. Change of shape of pendant liquid at the needle exit (dotted line) in (*a*) S1, (*b*) S3, (*c*) S6, (*d*) S9 and (*e*) S10 at $10^{-10}\,\mathrm{m^3\,s^{-1}}$ and 10 kV.

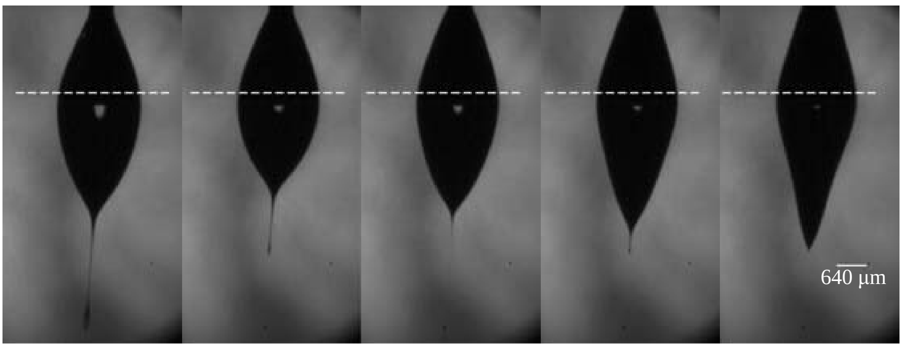

FIGURE 8. Change of shape of pendant liquid at the needle exit in S10 on increasing applied voltage from 10 kV to 14 kV at $10^{-10}\,\mathrm{m^3\,s^{-1}}$.

the non-dimensional jet diameter is smaller and the corresponding equations for flow rates of 10^{-10} and $10^{-12}\,\mathrm{m^3\,s^{-1}}$ are

$$J_{d10} = 0.02oh + 0.004, \tag{1a}$$

$$J_{d12} = 0.008oh + 0.004, \tag{1b}$$

where J_{d10} and J_{d12} are the non-dimensional jet diameters for the flow rate of 10^{-10} and $10^{-12}\,\mathrm{m^3\,s^{-1}}$, respectively.

The shape of the pendant liquids at the exit of the needle also changes with viscosity. With increasing viscosity, it becomes deeper as shown in figure 7. This was also found by Watanabe, Matsuyama & Yamamoto (2003) for conducting liquids. Figure 8 illustrates how the shape of the pendant liquid at the exit of the needle changes with applied voltage, where increase in applied voltage increases the electrical stresses and elongates the pendant liquid, changing the shape from parabolic to triangular.

Electric charges are induced at the surface of the meniscus and as the applied voltage was gradually increased the charges build up and eventually result in the unsteady transient jet. We define the dimensionless charging current as $I = I/I_0$, where $I_0 = (\varepsilon_0\sigma^2/\rho)^{1/2} \approx 2\times10^{-9}$ nA (Ganan-Calvo *et al.* 1997; Higuera 2004). I increases with the Ohnesorge number (figure 9) because a larger liquid meniscus prevails as viscosity increases. The charging current also increases with increasing flow rate and this is consistent with the fact that a larger meniscus and jet diameter occurs at higher

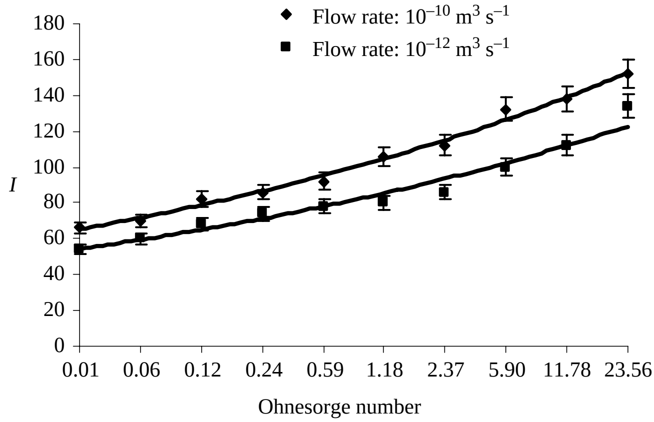

FIGURE 9. The variation of non-dimensional charging current (I) with Ohnesorge number at $10^{-10}\,\mathrm{m^3\,s^{-1}}$ and $10^{-12}\,\mathrm{m^3\,s^{-1}}$, 10 kV.

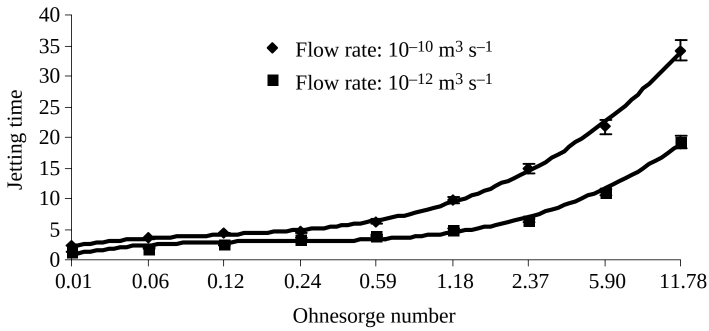

FIGURE 10. The variation of non-dimensional time elapsed between start and finish of jetting (J_t) with Ohnesorge number.

flow rates. The relationships between the current and Ohnesorge number are

$$I_{10} = 59.5\mathrm{e}^{0.094oh}, \tag{2a}$$

$$I_{12} = 49.6\mathrm{e}^{0.091oh}, \tag{2b}$$

where I_{10} and I_{12} are the non-dimensional charging currents for flow rates of $10^{-10}\,\mathrm{m^3\,s^{-1}}$ and $10^{-12}\,\mathrm{m^3\,s^{-1}}$, respectively.

The frequency of unsteady jetting of these silicone oils is much lower than that for liquids undergoing EHDA (Jaworek & Krupa 1999). At a set applied voltage and flow rate, a finite time lapses before a jet is ejected from the cone apex. This is because t_e is very large compared with conducting liquids, therefore it takes a longer time for the charge to reach the surface of the liquid and for the electrical stresses to take effect. The jetting time t_j, defined as the time taken for jetting to start and finish, shown in figure 4, increases with increasing viscosity and this phenomenon is quantified in figure 10, where non-dimensional jetting time is defined as $J_t = t_j/t_c$. Since the *other* properties of the silicone oils, except the viscosity, are nearly equal, forces, such as the liquid pressure, gravity, surface tension, inertia and electrical stresses, acting on the liquid surface of each silicone oil are approximately the same. The viscosity force prevents liquid from flowing and therefore it is the reason for the longer jetting time at a higher viscosity. At higher flow rates, e.g. $10^{-10}\,\mathrm{m^3\,s^{-1}}$ compared with $10^{-12}\,\mathrm{m^3\,s^{-1}}$,

J_t is larger (figure 10). The relationship between J_t and Ohnesorge number fits the following equations:

$$J_{t10} = 0.11oh^3 - 0.94oh^2 + 3.22oh - 0.090, \tag{3a}$$

$$J_{t12} = 0.10oh^3 - 1.13oh^2 + 4.23oh - 2.38, \tag{3b}$$

where J_{t10} and J_{t12} are the non-dimensional jetting times for flow rates of $10^{-10}\,\mathrm{m^3\,s^{-1}}$ and $10^{-12}\,\mathrm{m^3\,s^{-1}}$, respectively.

4. Conclusions

This study shows that in the family of dielectric liquids with electrical conductivity $\sim 10^{-13}\,\mathrm{S\,m^{-1}}$, only unsteady jets can be generated. The onset of unsteady transient jetting is characterized using the charging current. The experimental data show that the jet diameter increases linearly with increase in Ohnesorge number, and at lower flow rates the jet diameter is smaller. The shape of the pendant liquid at the exit of the needle elongates with increasing viscosity, and on increasing the applied voltage its shape changes from parabolic to triangular. The time elapsed between the start and finish of the unsteady jet increases with increasing Ohnesorge number, the trend fitting a third-order polynomial, and at lower flow rates this time span is smaller.

EPSRC (UK) is gratefully acknowledged for funding this research (Grant GR/T 01600). Mr Adrian Hamlin from Glassman Europe Ltd. is thanked for advice given on the measurement of the transient current.

REFERENCES

Balachandran, W. & Machowski, W. 1998 Electrohydrodynamic atomization of insulating liquids. *IEEE* **203** (ISSN 0-7803-5035-9).

Chen, D. R. & Pui, D. Y. H. 1997 Experimental investigation of scaling laws for electrospraying: Dielectric constant effect. *Aerosol Sci. Tech.* **27**, 367.

Fenn, J. B., Mann, M., Meng, C. K., Wong, S. F. & Whitehouse, C. M. 1989 Electrospray ionization for mass spectrometry of large biomolecules. *Science* **246**, 64.

Galicki, D., Berezin, A. A. & Chang, J. S. 1996 Electrohydrodynamic atomization of dielectric liquids. *IEEE Annu. Rep.* **365**.

Ganan-Calvo, A. M., Davila, J. & Barrero, A. 1997 Current and droplet size in the electrospraying of liquids. Scaling laws. *J. Aerosol Sci.* **28**, 249.

Gomez, A., Bingham, D., Juan, L. D. & Tang, K. 1998 Production of protein nanoparticles by electrospray drying. *J. Aerosol Sci.* **29**, 561.

Higuera, F. J. 2004 Current/flow-rate characteristic of an electrospray with a small meniscus. *J. Fluid Mech.* **513**, 239.

Jayasinghe, S. N. & Edirisinghe, M. J. 2002 A novel method of forming open cell ceramic form. *J. Porous Mater.* **9**, 265.

Jayasinghe, S. N. & Edirisinghe, M. J. 2004*a* Electrically-field driven jetting from dielectric liquids. *App. Phys. Lett.* **85**, 4243.

Jayasinghe, S. N. & Edirisinghe, M. J. 2004*b* Electrically forced jets and microthreads of high viscosity dielectric liquids. *J. Aerosol Sci.* **35**, 233.

Jayasinghe, S. N. & Edirisinghe, M. J. 2005 Electrostatic atomization of a ceramic suspension at pico-flow rates. *Appl. Phys.* A **80**, 399.

Jaworek, A. & Krupa, A. 1999 Classification of the modes of EHD spraying. *J. Aerosol Sci.* **30**, 873.

Ku, B. K. & Kim, S. S. 2002 Electrospray characteristics of highly viscous liquids. *J. Aerosol Sci.* **33**, 1361.

Li, K. Y., Tu, H. H. & Ray, A. K. 2005 Charge limits on droplets evaporation. *Langmuir* **21**, 3786.

Lopez-Herrera, J. M. & Ganan-Calvo, A. M. 2004. A note on charged capillary jet breakup of conducting liquids: experimental validation of a viscous one-dimensional model. *J. Fluid Mech.* **501**, 303.

McKinley, H. G. 2005 Non-dimensional group for understanding free surface flows of complex fluid. *SOR Rheology Bull.*

Rosell-Llompart, J. & Fernández de la Mora, J. 1994 Generation of monodisperse droplets 0.3 to 4 μm in diameter from electrified cone-jets of highly conducting and viscous liquids. *J. Aerosol Sci.* **25**, 1093.

Watanabe, H., Matsuyama, T. & Yamamoto, H. 2003 Experimental study on electrostatic atomization of highly viscous liquids. *J. Electrost.* **57**, 183.